Characterizing PID Controllers for Linear Time-Delay Systems: A Parameter-Space Approach

Xu-Guang Li, Silviu-Iulian Niculescu, *Fellow, IEEE*, Jun-Xiu Chen, and Tianyou Chai, *Fellow, IEEE*

***Abstract*—We focus on the proportional-integral-derivative (PID) controller design for linear time-delay systems. All the controller gains (k_P, k_I, and k_D) and the delay (τ) are treated as free parameters and no particular constraints are imposed on the controlled plants. Such a problem (involving totally four free parameters) is of theoretical as well as practical importance, but, to the best of the authors' knowledge, it has not been fully explored. First, we will develop an algebraic algorithm to solve the complete stability problem w.r.t. τ. Consequently, for any given PID controller vector (k_P, k_I, k_D), the distribution of $NU(\tau)$ ($NU(\tau)$ denotes the number of characteristic roots in the right-half plane, as a function of τ) can be accurately obtained and the exhaustive stability range of τ may be automatically calculated. Next, a global understanding of the distribution of $NU(\tau)$ over the whole (k_P, k_I, k_D)-space may be achieved and all structural changes regarding the $NU(\tau)$ distribution can be analytically determined. To achieve such a goal, a complete positive real root classification (for some appropriate auxiliary characteristic equation) will be explicitly proposed. Finally, we will give a new methodology, a new parameter-space approach, for determining the stability set in the (k_P, k_I, k_D, τ)-space.**

***Index Terms*—Asymptotic behavior analysis, complete positive real root classification, complete stability analysis, proportional-integral-derivative (PID) controllers, time-delay systems.**

Manuscript received December 29, 2019; revised August 5, 2020; accepted October 4, 2020. Date of publication October 13, 2020; date of current version September 27, 2021. This work was supported by National Natural Science Foundation of China under Grant 61733003. Recommended by Associate Editor C.-Y. Kao. *(Corresponding author: Xu-Guang Li.)*

Xu-Guang Li and Jun-Xiu Chen are with the State Key Laboratory of Synthetical Automation for Process Industries, and School of Information Science and Engineering, Northeastern University, Shenyang 110819, China (e-mail: masdanlee@163.com; chenjunxiu1024@163.com).

Silviu-Iulian Niculescu is with the Laboratoire des Signaux et Systèmes (L2S, UMR CNRS 8506), CNRS-CentraleSupélec-Université Paris-Sud, 91192 Gif-Sur-Yvette, France (e-mail: Silviu.Niculescu@l2s.centralesupelec.fr).

Tianyou Chai is with the State Key Laboratory of Synthetical Automation for Process Industries, Northeastern University, Shenyang 110819, China (e-mail: tychai@mail.neu.edu.cn).

Color versions of one or more of the figures in this article are available online at https://ieeexplore.ieee.org.

Digital Object Identifier 10.1109/TAC.2020.3030860

I. Introduction

THE proportional-integral-derivative (PID) controller design for time-delay systems is a classical problem (see, e.g., [29]). On the one hand, PID controllers are used in more than 95% of industrial processes [2]. On the other hand, time-delay phenomena exist in almost all practical control systems (see, e.g., [7] and [20]).

Consider a single-input single-output (SISO) controlled plant with the transfer function

$$H_0(\lambda) = \frac{H_{\mathrm{N}}(\lambda)}{H_{\mathrm{D}}(\lambda)} \tag{1}$$

where $H_{\mathrm{D}}(\lambda)$ and $H_{\mathrm{N}}(\lambda)$ are coprime polynomials of λ with real coefficients. Without any loss of generality, $H_{\mathrm{D}}(\lambda)$ and $H_{\mathrm{N}}(\lambda)$ can be described as

$$H_{\mathrm{D}}(\lambda) = a_0 + a_1\lambda + \cdots + a_{\mathrm{n}}\lambda^{\mathrm{n}}, a_{\mathrm{n}} \neq 0$$

$$H_{\mathrm{N}}(\lambda) = b_0 + b_1\lambda + \cdots + b_{\mathrm{m}}\lambda^{\mathrm{m}}, b_{\mathrm{m}} \neq 0$$

with $\mathrm{n} \geq \mathrm{m}$. In practice, the control loop is subject to a delay τ, and the actual transfer function is expressed as $H_0(\lambda)e^{-\tau\lambda}$.

In this article, we employ the PID controller of the form

$$k_P + \frac{k_I}{\lambda} + k_D\lambda \tag{2}$$

where the controller gains k_P, k_I, and k_D are real parameters.

Our objective is to design PID controllers and to explicitly compute the corresponding exhaustive stability range of τ of the closed-loop system. Toward this end, we treat all the controller gains and the delay as *free parameters* simultaneously. To the best of the authors' knowledge, although such a problem involving totally *four free parameters* (k_P, k_I, k_D, and τ) has been largely treated, it has not received a complete characterization. One of the technical difficulties is related to the appearance of multiple and/or degenerate critical imaginary roots (CIRs) depending on the system parameters.

In the sequel, we briefly review some existing results concerning the PID stabilization for time-delay systems. A large body of results has been reported in the case of a fixed τ (see, e.g., [8], [23], [27], and [29]). Such a problem falls in the so-called D-decomposition problem [24]. By using the methods reported in the abovementioned references, all the stabilizing set for (k_P, k_I, k_D) can be obtained. Next, the pole assignment is investigated in [31], where the dominant poles with a fixed τ

may be assigned to some desired positions through adjusting the PID controller parameters. For generic systems with fixed delays, the continuous pole placement is presented in [19] and the spectral abscissa optimization is discussed in [18] and [21] (see also [20, Ch. 7]).

However, the aforementioned results cannot be applied when the delay τ is also a *free parameter*. Next, we recall some stabilization results for such a case. In the literature, a stability interval of τ in the form

$$\tau \in [0, \overline{\tau}) \tag{3}$$

is widely studied (stability robustness w.r.t. "small" delays), and the corresponding $\overline{\tau}$ is called the delay margin (see, e.g., [7] and [20]). In [10] and [22], the upper bound for $\overline{\tau}$ is estimated. While in [28], the lower bound for $\overline{\tau}$ is estimated. The lower bound is usually more useful for practical applications. For a lower bound τ_L, there exists a linear time-invariant (LTI) controller stabilizing the plant for $\tau \in [0, \tau_L)$.

Although the aforementioned results are very insightful, some limitations are as follows.

1) The stabilization conditions are sufficient but not necessary.
2) It is not easy to find the corresponding controllers, with which the upper/lower stabilizable bounds may be approached.
3) The required controllers are often complex (two such controllers can be seen in Example 8).
4) The stabilization set for τ is restricted to the form (3).

In this article, we will show that *a plant may be stabilized with more than one interval including or excluding 0*.

The *delay-independent* stabilization problem is investigated in, e.g., [1], [6], [9], and [25]. As the main technical issue is to ensure that there is no CIR for any τ, the delay τ is not treated as a free parameter.

As far as we know, the stabilization problem addressed in this article has not been fully investigated (though the existing algorithms cover some case studies). In this article, we will develop a new methodology to characterize the stability set in the (k_P, k_I, k_D, τ)-space. No constraint on the controlled plant (1) is imposed and arbitrarily complex asymptotic behavior of the CIRs is allowed. Our development consists of the following two stages.

i) The first stage is to study the complete stability problem w.r.t. τ under given (k_P, k_I, k_D). We will begin with the asymptotic behavior analysis through addressing the positive real roots of the auxiliary characteristic equation (termed the effective W roots in this article). Then, some algebraic results will be derived such that the distribution of $NU(\tau)$ can be precisely determined. Based on the $NU(\tau)$ distribution, we will develop a computationally efficient algorithm, by which the exhaustive stability range of τ can be obtained automatically. With the results derived at this stage, the stability problem in the 4-D (k_P, k_I, k_D, τ)-space can be transformed to the complete stability problem in the 3-D (k_P, k_I, k_D)-space.

ii) In the second stage, we will propose an approach to obtain the complete effective W root classification in the whole (k_P, k_I, k_D)-space. This classification is essential: As (k_P, k_I, k_D) continuously changes, the structure of $NU(\tau)$ expression varies iff the effective W root classification varies. With the complete effective W root classification, we may appropriately divide the (k_P, k_I, k_D)-space and the boundaries of different regions can be analytically determined. It should be pointed out that a full stability set characterization cannot be done without the results at this stage. As explained in the article, the $NU(\tau)$ distribution undergoes an abrupt change at the boundaries of different regions (divided according to the complete effective W root classification). Such boundaries are strongly connected to multiple effective W roots and their detection is not straightforward. Therefore, a dedicated "global" study of the parameter space is necessary.

Based on the abovementioned results, we will establish a parameter-space approach to determine the stability set in (k_P, k_I, k_D, τ)-space. Consequently, we can design the PID controller with the entire stability τ-set accurately computed.

This article is organized as follows. In Section II, some preliminaries and prerequisites are given. An algebraic algorithm for obtaining the whole stability range of τ, under fixed controller gains, is proposed in Section III. In Section IV, the complete effective W root classification is investigated. Some simplifications for the complete stability analysis and the complete effective W root classification are proposed in Section V. The parameter-space approach for determining the stability set in the (k_P, k_I, k_D, τ)-space is established in Section VI. Illustrative examples are provided in Section VII. Finally, this article concludes in Section VIII.

Notations: In this article, $\mathbb{R}$ ($\mathbb{R}_+$) denotes the set of (positive) real numbers and $\mathbb{C}$ is the set of complex numbers. For $\lambda \in \mathbb{C}$, $\mathrm{Re}(\lambda)$ and $\mathrm{Im}(\lambda)$ denote the real part and the imaginary part of λ, respectively. $\mathbb{C}_-$ ($\mathbb{C}_+$) denotes the left-half (right-half) plane; $\mathbb{C}_0$ is the imaginary axis; and $\mathbb{N}$ is the set of nonnegative integers. ε is a sufficiently small positive real number. For $\gamma \in \mathbb{R}$, $\lceil \gamma \rceil$ denotes the smallest integer greater than or equal to γ. Finally, $\deg(\cdot)$ denotes the degree of a polynomial.

II. Preliminaries and Prerequisites

When no confusion occurs, we let $k_I \neq 0$ in the context of PID controller (2). If $k_I = 0$, the PID controller (2) reduces to a PD controller (provided that $k_P \neq 0$ and $k_D \neq 0$).

For the closed-loop system of plant (1) subject to PID controller (2), the characteristic function is given by

$$f(\lambda, \tau) = H_{\mathrm{D}}(\lambda)\lambda + H_{\mathrm{N}}(\lambda)(k_I + k_P\lambda + k_D\lambda^2)e^{-\tau\lambda}. \tag{4}$$

The closed-loop system is asymptotically stable iff all the characteristic roots lie in $\mathbb{C}_-$.

We will not specifically consider a trivial case that $\lambda = 0$ is a characteristic root (this property holds for all $\tau \geq 0$). In this case ($b_0 = 0$), the closed-loop system cannot be asymptotically stable for any $\tau \geq 0$.

A. Some Elementary Principles

For the closed-loop system associated with characteristic function (4), there are three possible types: retarded, neutral, and advanced, i.e., when $\deg(H_{\mathrm{D}}(\lambda)\lambda) - \deg(H_{\mathrm{N}}(\lambda)(k_I + k_P\lambda + k_D\lambda^2)) > 0, = 0$, and < 0, respectively.

For a retarded-type (advanced-type) system, as τ increases from 0 to $+\varepsilon$, an arbitrarily small positive real number, infinitely many new characteristic roots appear at the far left (right) of the complex plane.

For a neutral-type system, as τ increases from 0 to $+\varepsilon$, infinitely many new characteristic roots appear between two vertical lines in the complex plane, and hence, the positions of the vertical lines lead to a necessary stability condition (the below constraints (5) and (7) are due to it). For more details, one may refer to [20, Sec. 1.2] or [12, Ch. 10].

We have three elementary principles for adopting the PID controller.

Elementary Principle 1: In the case $\deg(H_{\mathrm{D}}(\lambda)) \geq \deg(H_{\mathrm{N}}(\lambda)) + 2$, the PID controller (2) may be applied. The closed-loop system is of the retarded type.

Elementary Principle 2: In the case $\deg(H_{\mathrm{D}}(\lambda)) = \deg(H_{\mathrm{N}}(\lambda)) + 1$, the PID controller (2) may be applied. The closed-loop system is of the neutral type and the gain k_D has to satisfy the condition

$$|k_D| < \left|\frac{a_n}{b_m}\right|. \tag{5}$$

If $k_D = 0$, the PID controller reduces to a PI controller

$$k_P + \frac{k_I}{\lambda}. \tag{6}$$

The PI controller (6) may be used, under which the closed-loop system is of the retarded type.

Elementary Principle 3: In the case $\deg(H_{\mathrm{D}}(\lambda)) = \deg(H_{\mathrm{N}}(\lambda))$, the PID controller (2) with $k_D \neq 0$ cannot stabilize the plant. The PI controller (6) may be used. The closed-loop system is of the neutral type and the gain k_P has to satisfy the condition

$$|k_P| < \left|\frac{a_n}{b_m}\right|. \tag{7}$$

B. Complete Stability Problem w.r.t. Delay Parameter

For a given controller vector (k_P, k_I, k_D), the complete stability problem w.r.t. τ refers to the problem of studying the stability property along the whole nonnegative τ-axis.

By the root continuity argument, $NU(\tau)$ changes as τ increases only when the system has a CIR $\lambda = j\omega$, $\omega \in \mathbb{R}$, at some τ. These delays are called the critical delays (CDs). A pair (λ, τ), where $\lambda \in \mathbb{C}_0$ and $\tau \in \mathbb{R}_+ \cup \{0\}$, such that $f(\lambda, \tau) = 0$ is called a *critical pair*.

The generic solution for the complete stability problem consists of two tasks: first, an exhaustive detection of the CIRs and the CDs; and second, the asymptotic behavior analysis of the CIRs w.r.t. the infinitely many CDs. Due to the conjugate symmetry of the spectrum, it suffices to consider only the CIRs with nonnegative imaginary parts.

Without any loss of generality, suppose that there exist $u \in \mathbb{N}$ CIRs, denoted by $\lambda_\alpha = j\omega_\alpha, \alpha = 0, \ldots, u-1$. For a CIR $\lambda_\alpha = j\omega_\alpha$, the infinitely many CDs are denoted by $\tau_{\alpha,k} = \tau_{\alpha,0} + \frac{2k\pi}{\omega_\alpha}$, $k \in \mathbb{N}$, where $\tau_{\alpha,0}$ is the minimum nonnegative value of τ satisfying the condition

$$e^{-\tau\omega_\alpha j} = -\frac{H_{\mathrm{D}}(j\omega_\alpha)j\omega_\alpha}{H_{\mathrm{N}}(j\omega_\alpha)(k_I + k_P j\omega_\alpha - k_D\omega_\alpha^2)}. \tag{8}$$

Property 1: For the closed-loop system described by (1) and (2), a nonzero CIR only corresponds to one set of CDs.

Property 1 may be proved in the line of [14, Property 1].

For a critical pair $(\lambda_\alpha, \tau_{\alpha,k} > 0)$, the effect of its asymptotic behavior on $NU(\tau)$, can be quantified by means of the notation $\Delta NU_{\lambda_\alpha}(\tau_{\alpha,k}) \in \mathbb{N}$. As defined in [12], $\Delta NU_{\lambda_\alpha}(\tau_{\alpha,k})$ stands for the change of $NU(\tau)$ caused by the variation of the CIR λ_α as τ increases from $\tau_{\alpha,k} - \varepsilon$ to $\tau_{\alpha,k} + \varepsilon$.

III. Algorithm for Complete Stability Analysis Under Fixed Controller Parameters

The objective of this section is to develop some algebraic criteria for the complete stability analysis under any given (k_P, k_I, k_D). An algorithm such that the entire stability range of τ can be *automatically* computed will also be presented.

A. Auxiliary Characteristic Function

Following the line of [5, Sec. 2], we can straightforwardly have the following lemma.

Lemma 1: For given k_P, k_I, and k_D, $\lambda = j\omega \neq 0$ is a CIR for the closed-loop system described by (1) and (2) iff $W = \omega^2$ is a positive real root for the auxiliary characteristic equation $F_{\mathrm{PID}}(W) = 0$, where $F_{\mathrm{PID}}(W)$ is the auxiliary characteristic function given by

$$\begin{aligned} F_{\mathrm{PID}}(W) &= \mathrm{Re}(H_{\mathrm{D}}(j\omega)j\omega)^2 + \mathrm{Im}(H_{\mathrm{D}}(j\omega)j\omega)^2 \\ &\quad - \mathrm{Re}(H_{\mathrm{N}}(j\omega)(k_I + k_P j\omega - k_D\omega^2))^2 \\ &\quad - \mathrm{Im}(H_{\mathrm{N}}(j\omega)(k_I + k_P j\omega - k_D\omega^2))^2. \end{aligned} \tag{9}$$

The right-hand side of (9) is a polynomial of ω with only even orders, and hence, the auxiliary characteristic function may be denoted as a polynomial of $W = \omega^2$.

As we have precluded the case where $\lambda = 0$ is a characteristic root, we will not consider the case $F_{\mathrm{PID}}(0) = 0$. Since $W = \omega^2$, we are only interested in the positive real roots, called the *effective W roots*. Consistent with the CIRs, there are u effective W roots denoted by W_α, $\alpha = 0, \ldots, u-1$, with $W_\alpha = \omega_\alpha^2$.

The application of auxiliary characteristic function may be traced back to [5]. However, the existing methods have strong restrictions. It is pointed out in [32] that *it is an open issue to address the multiple auxiliary characteristic roots*. In the sequel, we will give some new results covering the open issue.

B. Asymptotic Behavior and Auxiliary Characteristic Roots

Without any loss of generality, suppose that among the effective W roots there are $q_o \in \mathbb{N}$ ($q_e \in \mathbb{N}$) ones with odd (even) multiplicities, denoted by $W_0^o, \ldots, W_{q_o-1}^o$ ($W_0^e, \ldots, W_{q_e-1}^e$). We arrange them as

$$W_0^o > \cdots > W_{q_o-1}^o > 0, W_0^e > \cdots > W_{q_e-1}^e > 0. \tag{10}$$

For each $W_i^\dagger$ ($\dagger$ is "o" or "e"), we denote the corresponding critical pairs by $(\lambda_i^\dagger = j\omega_i^\dagger, \tau_{i,k}^\dagger)$, where $\omega_i^\dagger = \sqrt{W_i^\dagger} > 0$ and $\tau_{i,k}^\dagger = \tau_{i,0}^\dagger + \frac{2k\pi}{\omega_i^\dagger}$ ($k \in \mathbb{N}$) are the associated CDs. In light of [14, Th. 2], we have the following algebraic criterion.

Theorem 1: For the closed-loop system described by (1) and (2) with given gains k_P, k_I, and k_D, the following two statements hold.

(1) For a CIR $\lambda_i^e = j\omega_i^e$, $\Delta NU_{\lambda_i^e}(\tau_{i,k}^e) = 0$ for all $\tau_{i,k}^e > 0$ ($k \in \mathbb{N}$).

(2) For a CIR $\lambda_i^o = j\omega_i^o$, $\Delta NU_{\lambda_i^o}(\tau_{i,k}^o) = +1$ (-1) for all $\tau_{i,k}^o > 0$ ($k \in \mathbb{N}$) if i is even (odd).

Next, based on Theorem 1, we can easily derive the expression of $NU(\tau)$ according to the root continuity argument.

Theorem 2: Consider the closed-loop system described by (1) and (2) with given k_P, k_I, and k_D. For any $\tau > 0$, which is not a CD, $NU(\tau)$ can be explicitly expressed as

$$NU(\tau) = NU(+\varepsilon) + \sum_{i=0}^{q_o-1} NU_i^o(\tau) \tag{11}$$

where

$$NU_i^o(\tau) = \begin{cases} 0, \tau < \tau_{i,0}^o, \\ (-1)^i 2\left\lceil \frac{\tau-\tau_{i,0}^o}{2\pi/\omega_i^o} \right\rceil, \tau > \tau_{i,0}^o, \end{cases} \text{if } \tau_{i,0}^o \neq 0$$

$$NU_i^o(\tau) = \begin{cases} 0, \tau < \tau_{i,1}^o, \\ (-1)^i 2\left\lceil \frac{\tau-\tau_{i,1}^o}{2\pi/\omega_i^o} \right\rceil, \tau > \tau_{i,1}^o, \end{cases} \text{if } \tau_{i,0}^o = 0.$$

(The value of $NU(+\varepsilon)$ can be calculated according to [12, Th. 5.1] or [13, Th. 1].)

Now, we can obtain the $NU(\tau)$ *distribution w.r.t. τ along the whole τ-axis*. Consequently, we may determine the whole stability range of τ through addressing the $NU(\tau)$ distribution.

Remark 1: The structure of $NU(\tau)$ is determined by the number of effective W roots and their respective multiplicities, in light of Theorems 1 and 2. This observation will play an important role in our global study of the parametric space.

In the following section, we will develop an algorithm by which all the stability range of τ can be *automatically* detected for a fixed (k_P, k_I, k_D).

C. Algebraic Algorithm for Complete Stability Analysis

Corollary 1: The closed-loop system described by (1) and (2) must belong to the following three cases.

1) Asymptotically stable for all $\tau \in [0, \infty)$.

2) Asymptotically stable along the whole τ-axis except at some isolated points.

3) There exists a $\tau^* \geq 0$ such that $NU(\tau) > 0$ for all $\tau \geq \tau^*$.

Case (1) happens iff $NU(0) = 0$ and there is no effective W root. Case (2) happens iff $NU(+\varepsilon) = 0$ and there are only effective W roots with even multiplicities. In the other situations, Case (3) occurs.

One may easily prove the abovementioned corollary by combining the idea of [12, Th. 9.2] (or [13, Th. 7]) and the algebraic results introduced previously in this section.

Based on Corollary 1, we will derive a computationally efficient algorithm for the complete stability analysis. Our idea is: Cases (1) and (2) can be easily determined according to the effective W roots and $NU(+\varepsilon)$. If these two cases are excluded, i.e., in Case (3), we may choose a sufficiently large τ^* and keep track of the finite-length $NU(\tau)$ distribution for $0 \leq \tau \leq \tau^*$. In this way, the exhaustive stability range of τ may be detected (details will be given in Algorithm 1).

When $\tau = 0$, the characteristic function (4) reduces to

$$f(\lambda, 0) = H_{\mathrm{D}}(\lambda)\lambda + H_{\mathrm{N}}(\lambda)(k_I + k_P\lambda + k_D\lambda^2). \tag{12}$$

All the $n+1$ characteristic roots can be computed by a computer, since (12) is an $(n+1)$th-order polynomial.

We define by $\mathcal{N}_{W+}^{\tau=0}$ the set in the (k_P, k_I, k_D)-space where there is at least one effective W root when $\tau = 0$ (i.e., the closed-loop system has CIRs when $\tau = 0$).

For a $(k_P, k_I, k_D) \notin \mathcal{N}_{W+}^{\tau=0}$, it is obvious that $NU(+\varepsilon) = NU(0)$. We now present the algorithm for the complete stability analysis for a $(k_P, k_I, k_D) \notin \mathcal{N}_{W+}^{\tau=0}$ (the case of $(k_P, k_I, k_D) \in \mathcal{N}_{W+}^{\tau=0}$ will be discussed in Section VI-A).

Algorithm 1 (complete stability analysis w.r.t. τ):

Step 1: Determine $NU(0)$ through solving the equation $f(\lambda, 0) = 0$, where $f(\lambda, 0)$ is given in (12).

Step 2: Solve the auxiliary characteristic equation $F_{\mathrm{PID}}(W) = 0$. If there is no effective W root, go to Step 3. If there are only effective W roots with even multiplicities, go to Step 4. Otherwise, go to Step 5.

Step 3: The closed-loop system is asymptotically stable (unstable) for all $\tau \in [0, \infty)$ if $NU(0) = 0$ (> 0). Go to Step 6.

Step 4: The closed-loop system is asymptotically stable along the whole τ-axis except at the CDs if $NU(0) = 0$. The closed-loop system cannot be asymptotically stable at any τ if $NU(0) > 0$. Go to Step 6.

Step 5: Choose a sufficiently large $\tau^* > 0$. Obtain all the critical pairs (λ, τ) where the CDs are not larger than τ^*. These CDs divide $[0, \tau^*]$ into finitely many open intervals. At all these CDs, the corresponding values of $\Delta NU_\lambda(\tau)$ can be computed by Theorem 1. Then, using Theorem 2, we can determine the value of $NU(\tau)$ for each open interval. An open interval of τ with $NU(\tau) = 0$ is a stability interval. As a result, all the stability intervals of τ (if any) may be explicitly computed.

Step 6: The algorithm stops.

For the complete stability problem of time-delay systems, various approaches have been proposed, see, e.g., [5], [13], [26], and [30]. However, most of the existing results have technical limitations. Algorithm 1 covers the general case for the PID stabilization problem of time-delay systems (this will be demonstrated by various examples in Section VII) and, moreover, it will be used in the sequel for the scenario where the controller gains are also free parameters.

IV. Complete Effective W Root Classification

By using the results of the last section, for any PID controller vector (k_P, k_I, k_D), the $NU(\tau)$ distribution can be algebraically determined. Along this line, the stability analysis over the 4-D

(k_P, k_I, k_D, τ)-space may be recast into the complete stability analysis over the 3-D (k_P, k_I, k_D)-space.

Our next task is to have some global characterization concerning the $NU(\tau)$ distribution over the (k_P, k_I, k_D)-space. Remark 1 provides a path along analyzing how the number of effective W roots and their multiplicities change over the whole (k_P, k_I, k_D)-space. Such an analysis is called the complete effective W root classification.

The contribution of this section is two-fold: (1) The whole parameter space of (k_P, k_I, k_D) will be properly divided into some regions. In each region, the $NU(\tau)$ expression has a fixed structure. (2) The boundaries of different regions divided in the (k_P, k_I, k_D)-space, where the $NU(\tau)$ distribution undergoes an abrupt change, may be analytically determined.

We will develop an approach for the complete effective W root classification, by taking into account the characteristics of closed-loop system with PID controller. We first review a mathematical tool for polynomial algebra.

A. Discrimination System

For a real-coefficient polynomial

$$Q(y) = c_q y^q + c_{q-1} y^{q-1} + \cdots + c_0, c_q \neq 0 \tag{13}$$

the *root classification* refers to the information concerning the numbers and multiplicities of the distinct real and complex roots of $Q(y) = 0$.

The *complete root classification* of $Q(y)$ is the collection of its all possible root classifications, together with the conditions on the *parametric coefficients* such that each root classification is realized. The complete root classification can be systematically solved by a generic tool, called the *discrimination system* (see [33] and the references therein).

For the qth-order polynomial $Q(y)$ (13), the *discrimination matrix* is the following $2q \times 2q$ matrix M

$$= \begin{pmatrix} c_q & c_{q-1} & c_{q-2} & \cdots & c_0 & & & & \\ 0 & qc_q & (q-1)c_{q-1} & \cdots & c_1 & & & & \\ & c_q & c_{q-1} & \cdots & c_1 & c_0 & & & \\ & 0 & qc_q & \cdots & 2c_2 & c_1 & & & \\ & & & \vdots & \vdots & & & & \\ & & & & c_q & c_{q-1} & c_{q-2} & \ldots & c_0 \\ & & & & 0 & qc_q & (q-1)c_{q-1} & \ldots & c_1 \end{pmatrix}.$$

Let D_α denote the determinant of the submatrix of M formed by the first 2α rows and the first 2α columns for $\alpha = 1, \ldots, q$. The q-tuple $D = [D_1, \ldots, D_q]$ is called the *discriminant sequence* of $Q(y)$. According to the signs of $D_1, \ldots, D_q$, we have the *revised sign list* for $Q(y)$.

Proposition 1 (see[33]): If the revised sign list for $Q(y)$ has l nonvanishing elements and the number of sign changes is v, then $Q(y)$ has v pairs of distinct complex conjugate roots and $l - 2v$ distinct real roots.

If Proposition 1 is not sufficient for concluding on the complete root classification (more precisely, it may be insufficient to determine the multiplicity information), we construct the so-called Δ-*sequence* of $Q(y)$. Then, through analyzing the complete root classification of the Δ-sequence (by using Proposition 1), we may determine the complete root classification of $Q(y)$ (i.e., the multiplicity information can also be available). For more details, please refer to [33].

To summarize, for the polynomial $Q(y)$ (13), we may obtain a set of explicit expressions in terms of the coefficients, called the *discrimination system*, which determines all the possible cases on the numbers and multiplicities of the real roots.

B. Complete Effective W Root Classification

As the auxiliary characteristic function $F_{\text{PID}}(W)$ is an $(n+1)$th-order polynomial, the discriminant sequence is of the form

$$[D_1, \ldots, D_{n+1}]. \tag{14}$$

Applying the discrimination system, we can classify the distribution of real W roots in the (k_P, k_I, k_D)-space, i.e., obtain the complete real W root classification, and divide the whole (k_P, k_I, k_D)-space into regions accordingly. We denote them by $\mathcal{N}_W^{\{\cdot,\ldots,\cdot\}}$. For instance, "$\mathcal{N}_W^{\{1,1,1\}}$" denotes a region with three distinct simple real W roots; "$\mathcal{N}_W^{\{2,1\}}$" denotes a region with one double real W root plus one simple real W root; "$\mathcal{N}_W^{\{\}}$" denotes a region without a real W root.

Among the real W roots, we need to filter out the negative ones (since $W = \omega^2$). To this end, in this section, we will give a novel approach to obtain the complete effective W root classification, i.e., the complete positive real W root classification, in the (k_P, k_I, k_D)-space.

We start by examining where a real W root may change its sign (i.e., a negative real W root becomes a positive real W root or the other way) in the (k_P, k_I, k_D)-space. There must exist a critical state where $W = 0$ is an auxiliary characteristic root if a real W root changes its sign.

In view of (9), the following property is true.

Property 2: For the closed-loop system described by (1) and (2), there exists an auxiliary characteristic root $W \to 0$ iff $k_I \to 0$.

We have the main theorem of this section described as follows.

Theorem 3: For the closed-loop system described by (1) and (2), consider a region divided according to the complete real W root classification. If this region is separated by the set $k_I = 0$ in the (k_P, k_I, k_D)-space, then the effective W root classification does not change in each subregion of this region separated by the set $k_I = 0$. Otherwise, the effective W root classification does not change in the whole region.

Proof: If a (k_P, k_I, k_D)-point continuously changes in a region divided according to the complete real W root classification, all the real W roots keep their signs if this point does not intersect the set $k_I = 0$, by Property 2. ■

The set $k_I = 0$ is nothing but a line in the 2-D parameter space or a plane in the 3-D parameter space. In light of Theorem 3, we have a computationally efficient procedure for the complete effective W root classification.

Procedure 1 (complete effective W root classification):

Step 1: Apply the discrimination system to the auxiliary characteristic function $F_{\text{PID}}(W)$. The complete real W root classification in the whole (k_P, k_I, k_D)-space can be obtained.

Step 2: For each region divided according to the complete real W root classification, we determine all possible effective W root classifications in light of Theorem 3. More precisely, for each region not separated by the set $k_I = 0$ (subregion separated by the set $k_I = 0$), we choose any point to solve the auxiliary characteristic equation $F_{\text{PID}}(W) = 0$ and the effective W root classification at this point is exactly the same as for all the points in the region (subregion).

Moreover, the analytic boundaries of different effective W root classifications in the (k_P, k_I, k_D)-space are available and can be explicitly computed (see the analysis in detail in Section IV-C).

Remark 2: An alternative way for the complete effective W root classification is: Let $W = V^2$ and then analyze the complete real V root classification for $F_{\text{PID}}(V^2) = 0$. However, the computational complexity for employing the discrimination system substantially increases. Procedure 1 combines the discrimination system and the characteristics of the closed-loop system with PID controller. This procedure considerably reduces the computational complexity.

In the sequel, we introduce *underlines* and *overlines* to the notation $\mathcal{N}_W^{\{\cdot,\ldots,\cdot\}}$ to clarify the sign of each real W root. Furthermore, we denote the regions divided according to the complete effective W root classification by $\mathcal{N}_{W_+}^{\{\cdot,\ldots,\cdot\}}$. For instance: If a region $\mathcal{N}_W^{\{1,1,1\}}$ (with three distinct simple real W roots) is with two simple *negative* real W roots and one simple *positive* real W root, we denote this region by "$\mathcal{N}_W^{\{\underline{1},\underline{1},\overline{1}\}}$" or "$\mathcal{N}_{W_+}^{\{1\}}$" (with one simple *effective* W root); if a region $\mathcal{N}_W^{\{2,1\}}$ (with one double real W root plus one simple real W root) is with one double *positive* real W root and one simple *negative* real W root, we denote this region by "$\mathcal{N}_W^{\{\overline{2},\underline{1}\}}$" or "$\mathcal{N}_{W_+}^{\{2\}}$" (with one double *effective* W root).

The above description may by further simplified by introducing an arrow "$\rightarrow$". For instance, we may simply use "$\mathcal{N}_W^{\{1,1,1\}} \rightarrow \mathcal{N}_W^{\{\underline{1},\underline{1},\overline{1}\}} \rightarrow \mathcal{N}_{W_+}^{\{1\}}$" and "$\mathcal{N}_W^{\{2,1\}} \rightarrow \mathcal{N}_W^{\{\overline{2},\underline{1}\}} \rightarrow \mathcal{N}_{W_+}^{\{2\}}$" to summarize the two cases in the last paragraph.

C. Boundaries of Different Effective W Root Classifications

We first give a useful property as follows.

Property 3: For the closed-loop system described by (1) and (2), as (k_P, k_I, k_D) continuously varies, the effective W root classification changes iff the (k_P, k_I, k_D)-point intersects a region with multiple effective W roots or the plane $k_I = 0$.

Proof: The characteristic function (4) is with real coefficients, and hence, all the complex W roots appear in complex conjugate pairs. As (k_P, k_I, k_D) continuously varies, if the effective W root classification changes, the following cases are possible.

Case (1): The total number of effective W roots (multiplicity taken into account) changes. More precisely, Case (1) has two subcases.

Subcase (1.1): A pair of complex conjugate W roots collide on the real axis (a double effective W root appears and the total number of effective W roots increases by two) or a double effective W root splits into two complex conjugate W roots (a double effective W root disappears and the total number of effective W roots decreases by two).

Subcase (1.2): A positive real W root becomes a $W = 0$ root (total number of effective W roots decreases by one) or a $W = 0$ root becomes a positive real W root (total number of effective W roots increases by one).

Case (2): The total number of effective W roots (multiplicity taken into account) does not change. However, the multiplicity information changes. Case (2) happens if real W roots collide or split along the real axis.

Subcase (1.1) and Case (2) happen on the set with multiple effective W roots. Subcase (1.2) occurs on the set $k_I = 0$, according to Property 2. ■

We next focus on the regions with multiple effective W roots.

Property 4: For the auxiliary characteristic equation $F_{\text{PID}}(W) = 0$, there are multiple effective W roots only if $D_{n+1} = 0$.

It is a generic property related with the discrimination system that there is a multiple (real or complex) root iff the last element of the discriminant sequence equals to 0 (one may prove it by contradiction). As D_{n+1} is a polynomial of k_P, k_I, and k_D, a region satisfying $D_{n+1} = 0$ is in general with measure 0 in the (k_P, k_I, k_D)-space.

We refer to a region at which the effective W root classification changes as *a boundary of different effective W root classifications*, because such a region can be interpreted as a boundary surface (transition) of different effective W root classifications, in light of the abovementioned analysis. We can obtain the analytic conditions of a boundary from the complete effective W classification, and hence, we are able to accurately determine a boundary, although with measure 0.

Remark 3: It is seen from the proof of Property 3 that for almost all closed-loop systems with PID controllers, there exist sets of (k_P, k_I, k_D) parameters that result in multiple real W roots. Since all the complex W roots appear in complex conjugate pairs, the collision (if any) of a pair of complex conjugate W roots, as (k_P, k_I, k_D) continuously changes, must occur on the real axis. This gives rise to at least a double real W root.

D. Effective W Root Classification and $NU(\tau)$ Distribution

Now, we know that the $NU(\tau)$ distribution may have the following two types of variations.

1) In a region divided according to the complete effective W root classification, the $NU(\tau)$ distribution continuously varies w.r.t. (k_P, k_I, k_D).

2) On the boundaries where the effective W root classification changes, the $NU(\tau)$ distribution has an abrupt change w.r.t. (k_P, k_I, k_D).

Remark 4: Owing to the complete effective W root classification proposed in this article, even if the $NU(\tau)$ distribution has an abrupt change, we are able to accurately detect it. Moreover, inside a region with the same effective W root classification, we may apply the *parameter-sweeping technique* to study the

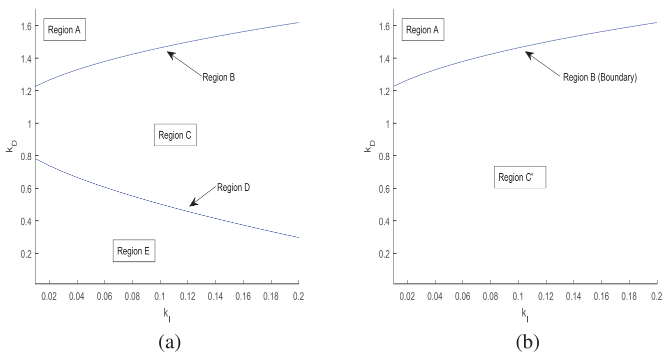

Fig. 1. Complete real and effective W root classifications for Example 1. (a) Real W root classifications. (b) Effective W root classifications.

$NU(\tau)$ distribution. It is worth mentioning that such a parameter sweeping is for the *quantitative* test.

Based on the results mentioned above, we will propose a systematic approach in Section VI to examine the stability set in the space of (k_P, k_I, k_D, τ). With the complete effective W root classification, the solution will be complete from the theoretical as well as the computational viewpoint.

E. Illustrative Explanatory Examples

Example 1: Consider the [28, controlled plant (40)]

$$H_0(\lambda) = \frac{1}{(\lambda - 0.2)(\lambda - 1)}.$$

Following the discussions in Section II-A, we employ the PID controller to this plant. For a clear illustration, we here analyze the case $k_P = -0.1$ and $(k_I, k_D) \in [0.01, 0.2] \times [0.01, 1.7]$. We now apply Procedure 1.

The auxiliary characteristic function is $F_{\mathrm{PID}}(W) = W^3 + (-k_D^2 + \frac{26}{25})W^2 + (-k_P^2 + 2k_I k_D + \frac{1}{25})W - k_I^2$.

Step 1: The discriminant sequence of $F_{\mathrm{PID}}(W)$ is $[D_1, D_2, D_3]$, where $D_1 = 3$, $D_2 = 2k_D^4 - \frac{104k_D^2}{25} - 12k_I k_D + 6k_P^2 + \frac{1202}{625}$, $D_3 = -4k_D^5 k_I k_P^2 + \frac{4k_D^5 k_I}{25} + \frac{104k_D^4 k_I^2}{25} + k_D^4 k_P^4 - \frac{2k_D^4 k_P^2}{25} + \frac{k_D^4}{625} + 4k_D^3 k_I^3 + \frac{208k_D^3 k_I k_P^2}{25} - \frac{208k_D^3 k_I}{625} + 30k_D^2 k_I^2 k_P^2 - \frac{6158k_D^2 k_I^2}{625} - \frac{52k_D^2 k_P^4}{25} + \frac{104k_D^2 k_P^2}{625} - \frac{52k_D^2}{15625} - \frac{936k_D k_I^3}{25} - 24k_D k_I k_P^4 - \frac{1504k_D k_I k_P^2}{625} + \frac{2104k_D k_I}{15625} - 27k_I^4 + \frac{468k_I^2 k_P^2}{25} + \frac{58604k_I^2}{15625} + 4k_P^6 + \frac{376k_P^4}{625} - \frac{1052k_P^2}{15625} + \frac{576}{390625}$.

Then, by using the discrimination system, we may divide the selected domain into the following regions [see Fig. 1 (a)]: Region A with $\mathcal{N}_W^{\{1,1,1\}}$: $D_2 > 0 \cap D_3 > 0$; Region B with $\mathcal{N}_W^{\{2,1\}}$: $D_2 > 0 \cap D_3 = 0$; Region C with $\mathcal{N}_W^{\{1\}}$: $(D_2 > 0 \cap D_3 < 0) \cup (D_2 = 0 \cap D_3 < 0) \cup (D_2 < 0 \cap D_3 < 0)$; Region D with $\mathcal{N}_W^{\{2,1\}}$: $D_2 > 0 \cap D_3 = 0$; Region E with $\mathcal{N}_W^{\{1,1,1\}}$: $D_2 > 0 \cap D_3 > 0$.

Step 2: For each region mentioned above, we may choose any point to determine the effective W root classification (the selected domain is not separated by the line $k_I = 0$). In practice, we do not need to specifically address the regions with measure 0, as the effective W root classifications may be implied from the ones of neighbouring regions. For this example, the effective W root classifications for Region B (Region D) can be implied from the ones of Regions A and C (Regions C and E).

According to Theorem 3, we have the complete effective W root classification: Region A: $\mathcal{N}_W^{\{1,1,1\}} \to \mathcal{N}_W^{\{\bar{1},\bar{1},\bar{1}\}} \to \mathcal{N}_{W_+}^{\{1,1,1\}}$; Region B: $\mathcal{N}_W^{\{2,1\}} \to \mathcal{N}_W^{\{\bar{2},\bar{1}\}} \to \mathcal{N}_{W_+}^{\{2,1\}}$; Region C: $\mathcal{N}_W^{\{1\}} \to \mathcal{N}_W^{\{\bar{1}\}} \to \mathcal{N}_{W_+}^{\{1\}}$; Region D: $\mathcal{N}_W^{\{2,1\}} \to \mathcal{N}_W^{\{\underline{2},\bar{1}\}} \to \mathcal{N}_{W_+}^{\{1\}}$; Region E: $\mathcal{N}_W^{\{1,1,1\}} \to \mathcal{N}_W^{\{\underline{1},\underline{1},\bar{1}\}} \to \mathcal{N}_{W_+}^{\{1\}}$.

Regions C–E may be combined into one region, denoted by Region C$' \triangleq$ Region C $\cup$ Region D $\cup$ Region E. As a consequence, we may divide the selected domain into three regions [see Fig. 1(b)]: Regions A–C$'$. Region B is the boundary between Regions A and C$'$, with the analytic condition: $D_2 > 0 \cap D_3 = 0$.

Finally, in Table I, we compare Procedure 1 with the standard method mentioned in Remark 2. It illustrates that Procedure 1 is more practical to implement. ■

TABLE I
COMPARISON OF COMPUTATIONAL COMPLEXITY

	$F_{\mathrm{PID}}(W)$	$F_{\mathrm{PID}}(V^2)$
Size of discrimination matrix	6×6	12×12
Discriminant sequence	$[D_1, D_2, D_3]$	$[D_1, \cdots, D_6]$
Maximum degree	8 (degree of D_3)	18 (degree of D_6)

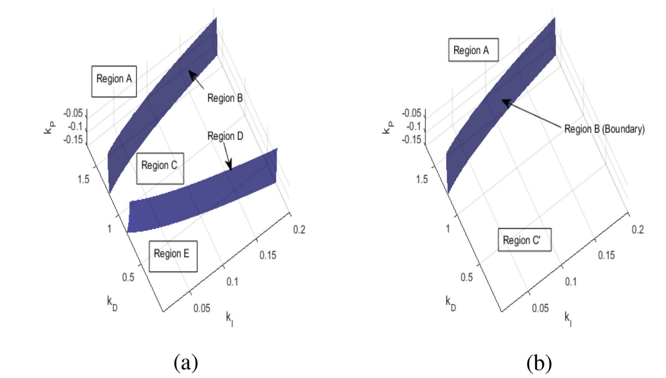

Fig. 2. Complete real and effective W root classifications for Example 2. (a) Real W root classifications. (b) Effective W root classifications.

Example 2: We now address the complete effective W root classification for the system of Example 1 over the 3-D (k_P, k_I, k_D)-space. For a clear illustration, we let $(k_P, k_I, k_D) \in [-0.15, -0.01] \times [0.01, 0.2] \times [0.01, 1.7]$.

By using Procedure 1, the domain may be divided into Regions A–E [see Fig. 2 (a)]: Region A: $\mathcal{N}_W^{\{1,1,1\}} \to \mathcal{N}_W^{\{\bar{1},\bar{1},\bar{1}\}} \to \mathcal{N}_{W_+}^{\{1,1,1\}}$; Region B: $\mathcal{N}_W^{\{2,1\}} \to \mathcal{N}_W^{\{\bar{2},\bar{1}\}} \to \mathcal{N}_{W_+}^{\{2,1\}}$; Region C: $\mathcal{N}_W^{\{1\}} \to \mathcal{N}_W^{\{\bar{1}\}} \to \mathcal{N}_{W_+}^{\{1\}}$; Region D: $\mathcal{N}_W^{\{2,1\}} \to \mathcal{N}_W^{\{\underline{2},\bar{1}\}} \to \mathcal{N}_{W_+}^{\{1\}}$; Region E: $\mathcal{N}_W^{\{1,1,1\}} \to \mathcal{N}_W^{\{\underline{1},\underline{1},\bar{1}\}} \to \mathcal{N}_{W_+}^{\{1\}}$. Regions C–E may be combined as Region C$' \triangleq$ Region C $\cup$ Region D $\cup$ Region E [see Fig. 2(b)].

We next verify the abovementioned results through choosing point "1" (in Region C$'$): $(k_P = -0.1, k_I = 0.1, k_D = 1.46404)$, point "2" (on Region B): $(k_P = -0.1,$

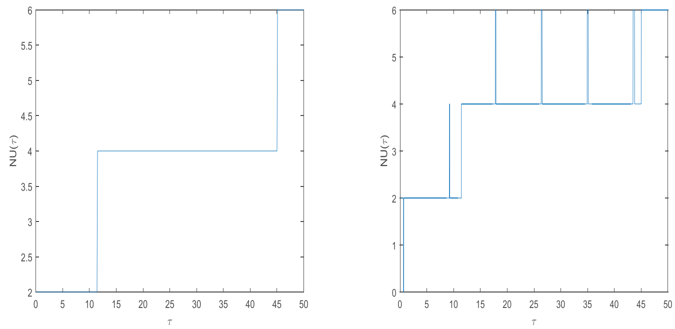

(a) (b)

Fig. 3. "$NU(\tau)$ versus τ" plots for Example 2. (a) At point "1." (b) At point "3."

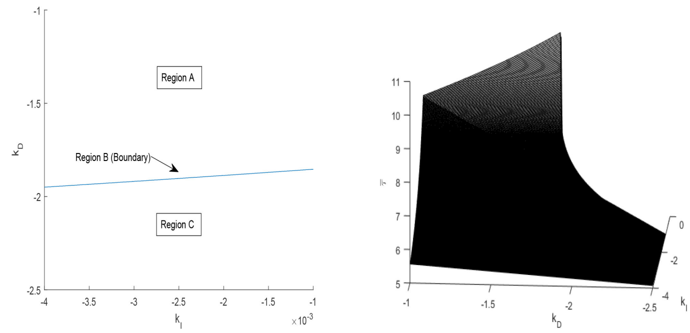

(a) (b)

Fig. 4. Complete effective W root classification and delay margin for Example 3. (a) Effective W root classification. (b) Delay margin.

$k_I = 0.1, k_D = 1.46405$), and point "3" (in Region A): $(k_P = -0.1, k_I = 0.1, k_D = 1.46406)$ to show the change of stability property caused by effective W root classifications. These three points represent the variation of (k_P, k_I, k_D) near $\mathcal{N}_{W_+}^{\{2,1\}}$ as k_D increases. At all of them $NU(0) = +2$, and hence, the difference of stability property is due to the effective W roots.

At point "1," there is only one simple effective W root 0.0350, and hence, the closed-loop system has no stability τ-interval. At point "2," there is one double effective W root 0.5342 and one simple effective W root 0.0350. The double W root is associated with a pair of degenerate CIRs $\lambda = \pm 0.7309j$: As τ increases near 0.6442, a pair of conjugate characteristic roots touch without crossing the imaginary axis $\mathbb{C}_0$ at $\pm 0.7309j$ in $\mathbb{C}_+$. This is a critical case that when $\tau = 0.6442$, the closed-loop system has a pair of conjugate characteristic roots in $\mathbb{C}_0$ but no characteristic roots in $\mathbb{C}_+$. At point "3," there are three simple effective W roots 0.5379, 0.5306, and 0.0350. As (k_P, k_I, k_D) varies from point "2" to point "3," the root loci touching the imaginary axis $\mathbb{C}_0$ (at point "2") *open a stability window* (at point "3"): At point "3," as τ increases near 0.64357 two conjugate characteristic roots cross $\mathbb{C}_0$ from right to left at $\pm 0.7284j$ while as τ increases near 0.64472 two conjugate characteristic roots cross $\mathbb{C}_0$ from left to right at $\pm 0.7334j$. The closed-loop system is asymptotically stable iff $\tau \in (0.64357, 0.64472)$.

An $NU(\tau)$ comparison between points "1" and "3" is made in Fig. 3 , where we see a structural change. ■

Example 3: Consider the [28, plant (42)]

$$H_0(\lambda) = \frac{0.1(0.1\lambda - 1)(\lambda + 0.1659)}{(\lambda - 0.1081)(\lambda^2 + 0.2981\lambda + 0.06281)}.$$

According to the discussions in Section II-A, we adopt the PID controller with $-100 < k_D < 100$. We now use Procedure 1 for the complete effective W root classification. For a clear illustration, we here choose a domain $(k_I, k_D) \in [-0.004, -0.001] \times [-2.5, -1.0]$ with $k_P = -0.4143$.

The auxiliary characteristic function is $F_{\mathrm{PID}}(W) = \chi_4 W^4 + \chi_3 W^3 + \chi_2 W^2 + \chi_1 W + \chi_0$, where $\chi_4 = 1 - \frac{k_D^2}{10000}$, $\chi_3 = -\frac{k_P^2}{10000} + \frac{k_I k_D}{10000} - (\frac{10002752281 k_D}{1000000000000} - \frac{k_I}{10000})k_D - \frac{1253539}{50000000}$, $\chi_2 = -\frac{10002752281 k_P^2}{1000000000000} - (\frac{2752281 k_D}{10000000000} - \frac{10002752281 k_I}{1000000000000})k_D + (\frac{10002752281 k_D}{1000000000000} - \frac{k_I}{10000})k_I + \frac{35155752614521}{10000000000000000}$, $\chi_1 = -\frac{2752281 k_P^2}{10000000000} + \frac{2752281 k_D k_I}{10000000000} + (\frac{2752281 k_D}{10000000000} - \frac{10002752281 k_I}{1000000000000})k_I + \frac{46100854437121}{10000000000000000000}$, $\chi_0 = -\frac{2752281 k_I^2}{10000000000}$.

Then, by Steps 1 and 2 of Procedure 1, we may obtain the complete effective W root classification. The selected domain may be divided into the following three regions [as depicted in Fig. 4 (a)]: Region A: $\mathcal{N}_{W_+}^{\{1\}}$; Region B: $\mathcal{N}_{W_+}^{\{2,1\}}$; Region C: $\mathcal{N}_{W_+}^{\{1,1,1\}}$.

For this example, the variation of the effective W root classification also causes a distinct change for the stability set. We here display how $\overline{\tau}$ varies w.r.t. k_I and k_D. Recall that $\overline{\tau}$ is the delay margin defined associated with (3), which is widely adopted as a stability/stabilization index in the literature. Using the methodology to be given later in this article, we obtain the result as shown in Fig. 4(b). One may notice the discontinuity of $\overline{\tau}$ w.r.t. (k_I, k_D). We now explain it from the angle of effective W root classification. Choose a nonself-intersecting continuous path in Fig. 4(a) and let (k_I, k_D) moves along this path from Region A to B (the boundary of Regions A and C) and then to Region C. Some details are given below as (k_I, k_D) is located in Regions A–C, respectively.

In Region A: As there is one simple effective W root and $NU(0) = 0$, the closed-loop system has one and only one stability τ-interval. On Region B: As (k_I, k_D) moves from Region A to B, an additional double effective W root appears, which corresponds to a critical pair (λ, τ) with $\Delta NU_\lambda(\tau) = 0$. For this example, it exhibits that, as (k_I, k_D) moves from Region A to B, a *breakpoint* appears in the stability τ-interval. In Region C: As (k_I, k_D) moves from Region B to C, the double effective W root splits into two distinct effective W roots [the corresponding two sets of critical pairs are with opposite signs for $\Delta NU_\lambda(\tau)$]. Consequently, as (k_I, k_D) moves from Region B to C, the *breakpoint* expands and thereby the original one stability τ-interval breaks into two. This causes a discontinuity (more precisely, an abrupt decrease) of $\overline{\tau}$, as shown in Fig. 4(b).

We choose $(k_I = -0.0012, k_D = -1.8609)$ and $(k_I = -0.0012, k_D = -1.8610)$ representing a point in Region A and a point in Region C, both close to the boundary Region B. The "$NU(\tau)$ versus τ" plots are given, respectively, in Fig. 5 (a)

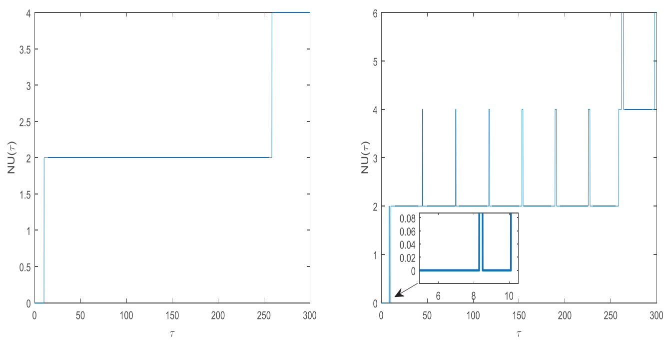

(a) (b)

Fig. 5. "$NU(\tau)$ versus τ" plots when $k_I = -0.0012$ for Example 3. (a) $k_D = -1.8609$. (b) $k_D = -1.8610$.

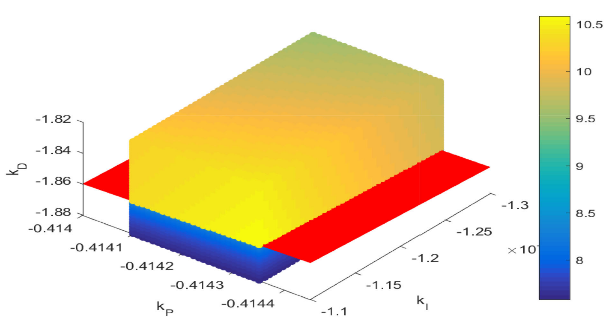

Fig. 6. Delay margin for Example 4.

and (b). It is seen that a very small change of k_D causes a structural variation of the $NU(\tau)$ distribution. ■

In order to have a more intuitive illustration for the qualitative change mentioned in Example 3, we next consider the case where k_P is also a free parameter near -0.4143.

Example 4: For the system in Example 3, the stability set in the (k_P, k_I, k_D, τ)-space will be studied in Example 8. We here specifically exhibit how the delay margin $\overline{\tau}$ varies w.r.t. (k_P, k_I, k_D) in Fig. 6, where the color information represents $\overline{\tau}$ and the red surface is the boundary $\mathcal{N}_{W_+}^{\{2,1\}}$. We can observe the *discontinuity* of $\overline{\tau}$ (a sharp change in color from dark to light), which occurs exactly on the boundary $\mathcal{N}_{W_+}^{\{2,1\}}$. ■

Remark 5: As illustrated in various examples in this article, there may be more than one stability τ-interval for the closed-loop system with PID controller. By using our approach, all stability τ-intervals can be precisely detected.

V. Further Algebraic Insights

In this section, we will specifically reduce the associated computation burden by further taking into consideration the characteristics of the closed-loop system with PID controller.

A. Improved Algebraic Algorithm

Theorem 2 requires the multiplicity information of the effective W roots, and it is used at Step 5 of Algorithm 1.

As summarized in Remark 4, the $NU(\tau)$ distribution can be globally characterized in the (k_P, k_I, k_D)-space, in light of the complete effective W root classification. In our methodology, Theorem 2 is used for a local analysis. In the sequel, we will present an improved version of Theorem 2.

For a controller vector (k_P, k_I, k_D), label all the effective W roots as $\widetilde{W}_0, \widetilde{W}_1, \ldots, \widetilde{W}_{\tilde{u}-1}$ ($\tilde{u}$ denotes the number of effective W roots, multiplicity taken into account) such that

$$\widetilde{W}_0 \geq \widetilde{W}_1 \geq \widetilde{W}_2 \geq \cdots. \tag{15}$$

For each $\widetilde{W}_\alpha$, we label a CIR $\tilde{\lambda}_\alpha = j\tilde{\omega}_\alpha$ ($\tilde{\omega}_\alpha^2 = \widetilde{W}_\alpha$) and denote the corresponding CDs by $\tilde{\tau}_{\alpha,k}$, $k \in \mathbb{N}$.

Theorem 4: Consider the closed-loop system described by (1) and (2) with given k_P, k_I, and k_D. For any $\tau > 0$, which is not a CD, $NU(\tau)$ can be explicitly expressed as

$$NU(\tau) = NU(+\varepsilon) + \sum_{i=0}^{\tilde{u}-1} \widetilde{NU}_i(\tau) \tag{16}$$

where

$$\widetilde{NU}_i(\tau) = \begin{cases} 0, \tau < \tilde{\tau}_{i,0}, \\ (-1)^i 2 \left\lceil \frac{\tau - \tilde{\tau}_{i,0}}{2\pi/\tilde{\omega}_i} \right\rceil, \tau > \tilde{\tau}_{i,0}, \end{cases} \text{if } \tilde{\tau}_{i,0} \neq 0$$

$$\widetilde{NU}_i(\tau) = \begin{cases} 0, \tau < \tilde{\tau}_{i,1}, \\ (-1)^i 2 \left\lceil \frac{\tau - \tilde{\tau}_{i,1}}{2\pi/\tilde{\omega}_i} \right\rceil, \tau > \tilde{\tau}_{i,1}, \end{cases} \text{if } \tilde{\tau}_{i,0} = 0.$$

The proof of Theorem 4 is given in Appendix A.

By using Theorem 4, we may determine the expression of $NU(\tau)$ without knowing the multiplicity information of the effective W roots.

Now, when employing Algorithm 1, Theorem 2 in Step 5 may be replaced by Theorem 4. In this way, the multiplicity information concerning the effective W roots is not explicitly required.

B. Symmetry Concerning Effective W Roots

First, it is not hard to see the following property for the coefficients of $F_{\text{PID}}(W)$.

Property 5: The coefficients of the auxiliary characteristic function $F_{\text{PID}}(W)$ (9) contain the terms k_P^2, k_I^2, k_D^2, and $k_I k_D$, without other terms involving k_P, k_I, or k_D.

Then, a useful result follows from Property 5:

Property 6: At a (k_P, k_I, k_D)-point, say $(\widehat{k}_P, \widehat{k}_I, \widehat{k}_D)$, all the W roots are preserved if $\widehat{k}_P$ is replaced by $-\widehat{k}_P$ and/or $(\widehat{k}_I, \widehat{k}_D)$ is replaced by $(-\widehat{k}_I, -\widehat{k}_D)$.

Thus, there is a symmetry concerning the effective W roots. Without loss of generality, consider a domain of the form: $(k_P, k_I, k_D) \in [-a, a] \times ([-b, 0) \cup (0, b]) \times [-c, c]$, where a, b, and c are positive real numbers (recall that $k_I \neq 0$ in context of PID controller). We have the following result.

Property 7: For the closed-loop system described by (1) and (2), the complete real W root classification for the domain $(k_P, k_I, k_D) \in [-a, a] \times ([-b, 0) \cup (0, b]) \times [-c, c]$ can be determined, if the complete real W root classification for the domain $(k_P, k_I, k_D) \in [0, a] \times (0, b] \times [-c, c]$ is known.

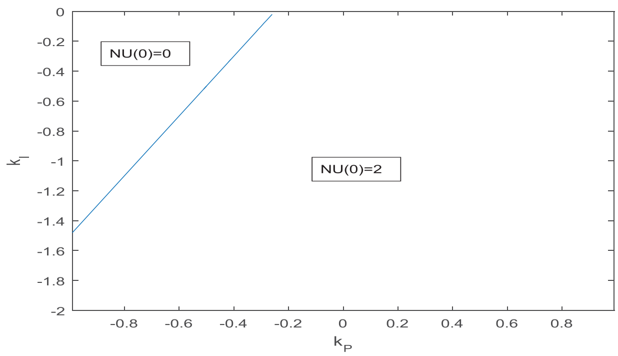

Fig. 7. $NU(0)$ versus (k_P, k_I) for Example 5.

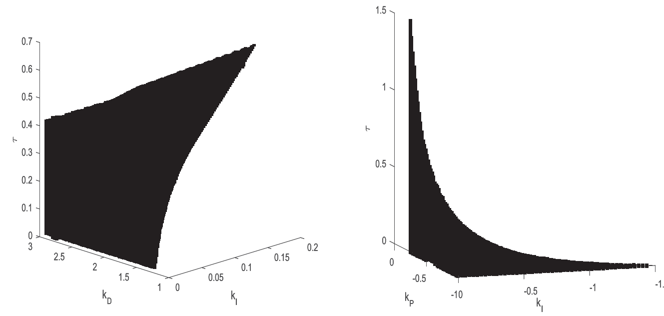

(a) (b)

Fig. 8. Stability sets for Examples 6 and 7. (a) Example 6. (b) Example 7.

Remark 6: Since a CIR $\lambda = j\omega$ is determined by $\omega^2 = W$, all the CIRs of the closed-loop system are not changed if we replace $\widehat{k}_P$ by $-\widehat{k}_P$ and/or $(\widehat{k}_I, \widehat{k}_D)$ by $(-\widehat{k}_I, -\widehat{k}_D)$. However, according to (8), the CDs are different.

Now, when employing Procedure 1, the domain to be examined for the complete real W root classification in the (k_P, k_I, k_D)-space can be quartered, in light of Property 7.

VI. Methodology for Examining Stability Set in (k_P, K_I, K_D, τ)-Space

In this section, we will give a new parameter-space approach for examining the stability set, with which the PID stabilization problem can be systematically solved.

In the sequel, we preclude the trivial case where the closed-loop system may be asymptotically stable independently of delay (the open-loop system is asymptotically stable, and the controller is not needed for the stabilization purpose).

A. On $NU(+\varepsilon)$ Analysis

The value of $NU(+\varepsilon)$ is required by Theorem 2 as well as Theorem 4. This calculation may be automatically finished by a computer if there is no CIR when $\tau = 0$.

Recall that we denote the set where the closed-loop system has CIRs when $\tau = 0$ by $\mathcal{N}_{W+}^{\tau=0}$. For a point in $\mathcal{N}_{W+}^{\tau=0}$, we may invoke the Puiseux series to determine the value of $NU(+\varepsilon)$ (according to [12, Th. 5.1] or [13, Th. 1]).

The set $\mathcal{N}_{W+}^{\tau=0}$ is in general with "measure 0" in the (k_P, k_I, k_D)-space (special cases, if any, may be tested according to the complete effective W root classification). In practice, we do not need to specifically analyze the set $\mathcal{N}_{W+}^{\tau=0}$. See the example as follows.

Example 5: Consider the [28, controlled plant (41)]

$$H_0(\lambda) = \frac{\lambda - 2}{\lambda - 0.5}.$$

Following the discussions in Section II-A, the PID controller is not applicable and we should apply the PI controller (6) with $-1 < k_P < 1$. The $NU(0)$ values w.r.t. k_P and k_I are given in Fig. 7 , where the boundary between the regions with $NU(0) = 0$ and $NU(0) = 2$ represents the set $\mathcal{N}_{W+}^{\tau=0}$.

We first analyze the set $\mathcal{N}_{W+}^{\tau=0}$ by a standard method (through [12, Th. 5.1] or [13, Th. 1]). For a point $(k_P = -0.5, k_I = -0.5)$ on the boundary, the characteristic equation when $\tau = 0$, $f(\lambda, 0) = 0$, has a pair of CIRs $\pm\sqrt{2}j$. We may analyze the asymptotic behavior through invoking the Taylor series at the critical pair $(\sqrt{2}j, 0)$: $\Delta\lambda = (2.0000 + 0.7071j)\Delta\tau + o(\Delta\tau)$, which implies that $NU(+\varepsilon) = 2$ at $(k_P = -0.5, k_I = -0.5)$. By the continuity, the closed-loop system is not asymptotically stable for a sufficiently small τ on the boundary.

In fact, the abovementioned result may be easily derived from the stability set, shown in Fig. 8 (b) (details will be given in Example 7). The border of the projection of the stability set on the (k_P, k_I)-plane is exactly the boundary in Fig. 7. ■

B. New Parameter-Space Approach

Parameter-Space Approach [Stability Set in (k_P, k_I, k_D, τ)-Space]:

Step 0: Select the controller type (PID or PI) according to the discussions in Section II-A.

Step 1: Obtain the complete effective W root classification, by using Procedure 1.

Step 2: Sweep the (k_P, k_I, k_D)-space and for each (k_P, k_I, k_D)-point, we study the complete stability problem using Algorithm 1.

Step 3: Display the stability set in the (k_P, k_I, k_D)-space. To be more precise: In the case of the PI controller, we display the stability set in the (k_P, k_I, τ)-space. In the case of the PID controller, we display the stability set through one or multiple colored figures in the (k_P, k_I, k_D)-space. For a (k_P, k_I, k_D)-point, the stability range of τ can be expressed by one or multiple colors.

For a given PID controller vector (k_P, k_I, k_D), if the stability τ-set is nonempty, without loss of generality, we suppose that it is consisted of s stability intervals

$$\tau \in (\underline{\tau}_1, \overline{\tau}_1) \cup \cdots \cup (\underline{\tau}_{\mathrm{s}}, \overline{\tau}_{\mathrm{s}}) \tag{17}$$

plus possible $\tau = 0$, with $0 \le \underline{\tau}_1 < \overline{\tau}_1 < \cdots < \underline{\tau}_{\mathrm{s}} < \overline{\tau}_{\mathrm{s}}$. We call $\overline{\tau}_{\mathrm{s}}$ in (17) the *generalized delay margin.*

In the subsequent colored figures, we will display the generalized delay margin via the color information.

Remark 7: One may exhibit more information concerning the stability intervals in the form (17) through more colored points, without any technical difficulty. As a consequence, the stability set in the (k_P, k_I, k_D, τ)-space may be displayed more comprehensively by multiple 3-D figures.

We now present three useful corollaries for some frequently-encountered cases. The explicit expression on *generalized delay margin* may be derived from these corollaries.

Corollary 2: If there is only one simple effective W root with $\widetilde{\tau}_{0,0} > 0$ and $NU(0) = 0$ ($NU(0) > 0$) in a region, then at each point in this region, the system is asymptotically stable iff $\tau \in [0, \widetilde{\tau}_{0,0})$ (there is no stability τ-interval).

Corollary 3: Suppose that there are two simple effective W roots, with $\widetilde{\tau}_{0,0} > 0$ and $\widetilde{\tau}_{1,0} > 0$, and $NU(0) = 0$ in a region. There are the following two possible cases at each point in this region.

1) If $\widetilde{\tau}_{1,0} \geq \widetilde{\tau}_{0,1}$, the system is asymptotically stable iff $\tau \in [0, \widetilde{\tau}_{0,0})$.

2) If $\widetilde{\tau}_{1,0} < \widetilde{\tau}_{0,1}$, there are multiple stability τ-intervals: $[0, \widetilde{\tau}_{0,0}) \cup (\bigcup_{k=0}^{\mathrm{N}} (\widetilde{\tau}_{1,k}, \widetilde{\tau}_{0,k+1}))$ with $\mathrm{N} = \sup\{k : \widetilde{\tau}_{0,k} < \widetilde{\tau}_{1,k} < \widetilde{\tau}_{0,k+1}\}$.

Corollary 4: Suppose that there are two simple effective W roots, with $\widetilde{\tau}_{0,0} > 0$ and $\widetilde{\tau}_{1,0} > 0$, and $NU(0) = 2$ in a region. There are the following three possible cases at each point in this region.

1) If $\widetilde{\tau}_{1,0} \geq \widetilde{\tau}_{0,0}$, there is no stability τ-interval.

2) If $\widetilde{\tau}_{1,0} < \widetilde{\tau}_{0,0}$ and $\widetilde{\tau}_{1,1} \geq \widetilde{\tau}_{0,1}$, the system is asymptotically stable iff $\tau \in (\widetilde{\tau}_{1,0}, \widetilde{\tau}_{0,0})$.

3) Otherwise, there are multiple stability τ-intervals: $\bigcup_{k=0}^{\mathrm{N}} (\widetilde{\tau}_{1,k}, \widetilde{\tau}_{0,k})$ with $\mathrm{N} = \sup\{k \geq 1 : \widetilde{\tau}_{0,(k-1)} < \widetilde{\tau}_{1,k} < \widetilde{\tau}_{0,k}\}$.

Based on the results of this article, one may prove the above-mentioned corollaries without any technical difficulty.

For the second case in Corollary 3 and the second and the third cases in Corollary 4, the generalized delay margin is larger than the "classical" delay margin (the delay margin may be zero even if there exists a stability τ-interval). For the other cases of the abovementioned Corollaries 2–4, the generalized delay margin and the delay margin are identical.

VII. Illustrative Examples

In this section, we will give some examples to illustrate the proposed parameter-space approach.

Example 6: Using our parameter-space approach, we here examine the stability set for the system considered in Example 1, with $k_P = -0.1$. The result is given in Fig. 8(a).

In the stability set [see Fig. 8(a)], $NU(0)$ may be positive. That is, the case where the plant cannot be stabilized when $\tau = 0$ is covered by our approach. Most of the stabilization approaches, e.g., [22] and [28], are not applicable in this case. ■

Remark 8: It is still a common technical limitation that "a time-delay system needs to be stabilizable when $\tau = 0$" in the existing stabilization studies. In addition, most of the existing results may be used to study only one stability τ-interval in the form (3). These restrictions are removed in this article.

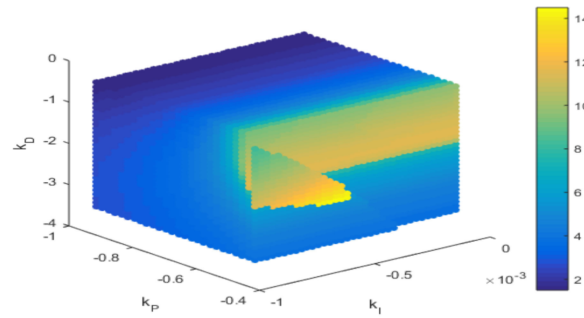

Fig. 9. Stability set for Example 8.

Example 7: For the controlled plant in Example 5, the lower stabilizable bound is about 1.5676 [28]. We now apply the parameter-space approach. As mentioned in Example 5, we employ the PI controller (6) with $-1 < k_P < 1$. The stability set is given in Fig. 8(b). ■

Example 8: Consider the controlled plant in Example 3. By using the approach of [28], two lower stabilizable bounds for τ are obtained as 15.4 and 12.6, with the following two required controllers, respectively

$$\frac{-1.506 \times 10^7 (\lambda + 0.1307)(\lambda^2 + 0.2664\lambda + 0.0204)}{(\lambda + 1103)(\lambda + 418.7)(\lambda + 3.376)(\lambda + 0.1778)} \times \frac{(\lambda^2 + 0.1582\lambda + 0.0303)(\lambda^2 + 0.2981\lambda + 0.0628)}{(\lambda + 0.1659)(\lambda + 0.1218)(\lambda^2 + 0.1885\lambda + 0.0333)}$$

$$\frac{6.016 \times 10^{-5} (\lambda + 0.275)(\lambda^2 + 0.2981\lambda + 0.0628)}{\lambda(\lambda + 0.1659)(\lambda + 10)(\lambda + 0.083 \times 10^6)}.$$

We now study the stability set under the PID controller, using the parameter-space approach. According to Step 0, we should employ the PID controller with $-100 < k_D < 100$. The stability set in the (k_P, k_I, k_D, τ)-space is obtained, as shown in Fig. 9. As mentioned, we use the color information to denote the generalized delay margin. It is worth mentioning that this system has more than one stability interval.

We find a controller vector $(k_P = -0.4143, k_I = -0.0006, k_D = -2.3050)$ with the stability set $[0, 5.4180) \cup (14.3769, 14.4952)$. That is, the maximum generalized delay margin is at least 14.4952. ■

Example 9: Consider a controlled plant

$$H_0(\lambda) = \frac{\lambda - \frac{1}{2}}{(\lambda - e^{\frac{\pi}{4}j})(\lambda - e^{-\frac{\pi}{4}j})}$$

which is the [28, controlled plant (45)]. The lower stabilizable bound is about 0.55 [28]. Using the parameter-space approach, we obtain the stability sets under PI and PID controllers, as shown in Fig. 10 (a) and (b). The maximum generalized delay margin is 0.7245 (1.2416) under the PI (PID) controller. ■

The computation time for obtaining the data of various figures in MATLAB (on a PC with an Intel Core 3.40 GHz CPU with 32 G RAM) is given in Table II. As we have mentioned above, the parameter sweeping in the parameter-space approach is for a quantitative analysis of the $NU(\tau)$ distribution and, hence, in practice we do not have to choose a very fine grid.

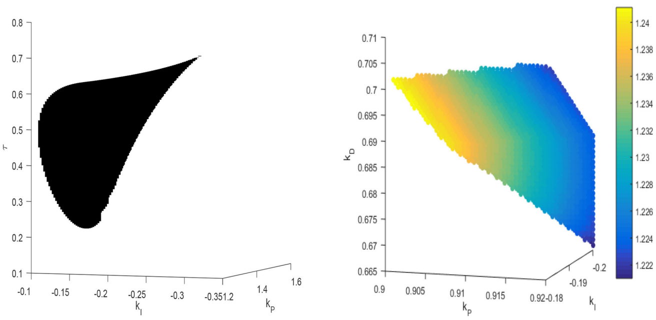

(a) (b)

Fig. 10. Stability sets for Example 9. (a) PI controller. (b) PID controller.

TABLE II
COMPUTATION TIME (SECONDS)

	Fig. 8(a)	Fig. 8(b)	Fig. 9	Fig. 10(a)	Fig. 10(b)
Time	0.071141	0.072166	4.209743	0.036372	1.202364

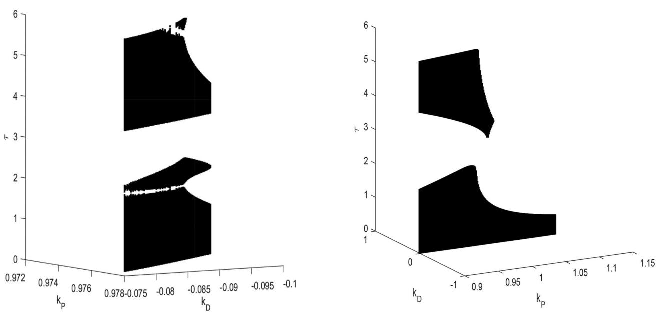

(a) (b)

Fig. 11. Stability set for Example 10. (a) Set with 3 and 4 stability τ-intervals. (b) Cross section $k_D = 0$.

Finally, we give two examples with the PD controller

$$k_P + k_D\lambda. \tag{18}$$

The characteristic function of the closed-loop system with PD controller (18) reads

$$f(\lambda,\tau) = H_{\mathrm{D}}(\lambda) + H_{\mathrm{N}}(\lambda)(k_P + k_D\lambda)e^{-\tau\lambda}. \tag{19}$$

Our approach is applicable to this case.

Example 10: Consider the plant with $H_{\mathrm{D}}(\lambda) = \lambda^5 + (\frac{\pi^2}{8} - \frac{\pi}{2} + 8)\lambda^4 + (-\frac{\pi}{2} + 3)\lambda^3 + (\frac{\pi^2}{4} - \pi + 10)\lambda^2 + (-\frac{\pi}{2} + 2)\lambda + \frac{\pi^2}{8} - \frac{\pi}{2} + 1$ and $H_{\mathrm{N}}(\lambda) = 8\lambda^4 + \lambda^3 + 10\lambda^2 + \lambda + 1$, which is borrowed from [11]. Here, we employ the PD controller (18).

First, following the discussions in Section II-A, we should confine $-\frac{1}{8} < k_D < \frac{1}{8}$. Then, using the parameter-space approach, we may obtain the stability set in the (k_P, k_D, τ)-space. In some region, there are multiple stability intervals of τ. Here, we specifically exhibit the part with three or four stability τ-intervals in Fig. 11 (a).

At $(k_P = 1, k_D = 0)$ there is a critical pair $(\lambda = j, \tau = \pi)$ with the Puiseux series $\Delta\lambda = 0.1468j(\Delta\tau)^{\frac{1}{2}} + (-0.0033 - 0.1473j)(\Delta\tau)^{\frac{2}{2}} + o((\Delta\tau)^{\frac{2}{2}})$. It implies that at $\tau = \pi$, the CIR $\lambda = j$ is double and degenerate. More interestingly, the asymptotic behavior has *a stabilizing effect:* As τ increases near π, *the appearance of this double CIR changes the stability property from being unstable to being asymptotically stable*.

As the asymptotic behavior of CIRs in general case may be analyzed by our approach, the analysis for point $(k_P = 1, k_D = 0)$ is included in the parameter-space approach, without any additional treatment. More precisely, for $(k_P = 1, k_D = 0)$, there are three effective W roots: $W_0 = 5.0268$ which is simple and with the critical pairs $(2.2421j, 1.2525 + 2.8024k)$, $W_1 = 1$ which is triple and with the critical pairs $(j, (2k+1)\pi)$, and $W_2 = 0.1115$ which is simple and with the critical pairs $(0.3339j, 5.8285 + 18.8155k)$. By using Algorithm 1, we have that the closed-loop system has two and only two stability intervals of τ: [0,1.2525) and $(\pi, 4.0549)$. For a clear illustration, we give the cross section $k_D = 0$ from the stability set in Fig. 11(b). ■

Remark 9: In characterizing the stability of time-delay systems, the asymptotic behavior analysis of multiple CIRs is a fundamental issue (see, e.g., [3], [4], [11], [13], and [17]). The abovementioned example shows that the appearance of a multiple CIR *may open a new stability interval of* τ. It is necessary to appropriately study the asymptotic behavior of multiple CIRs (otherwise, some stability intervals may be missing). As far as we know, none of the existing methods is valid for this case.

Finally, we consider the following second-order plant

$$H_0(\lambda) = \frac{1}{(\lambda - p_1)(\lambda - p_2)}. \tag{20}$$

Much attention has been paid to the stabilization of (20) subject to a delay τ, in the following three cases (see, e.g., [10], [15], [16], and [22]):

Case U.1: p_1 and p_2 are two positive real numbers.

Case U.2: p_1 and p_2 are a pair of conjugate complex numbers $\alpha \pm \beta j$ with $\alpha > 0$.

Case U.3: p_1 and p_2 are a pair of conjugate imaginary numbers $\pm j\omega_c$.

In a very recent paper [15], the exact delay margin for (20) controlled by the PID controller is studied, for Cases U.1–U.3. It is pointed out therein that in order to achieve the maximal delay margin, we should set $k_I = 0$ (i.e., use the PD controller).

Example 11: We first consider Case U.1 for (20) and list the maximal delay margin and the maximal generalized delay margin in Table III. Cases U.2 and U.3 can be addressed in the same way. In particular, for Case U.3 many stability τ-intervals can be found. For instance, if $p_1 = j$ and $p_2 = -j$, the maximal

TABLE III
MAXIMAL DELAY MARGIN AND MAXIMAL GENERALIZED DELAY MARGIN

	$p_1 = 0.6$ $p_2 = 0.8$	$p_1 = 1$ $p_2 = 1.2$	$p_1 = 0.4$ $p_2 = 2$
Maximal delay margin by approach in [15]	0.3960	0.2513	0.2595
Maximal generalized delay margin by approach in this paper	0.8304	0.5304	0.4497

delay margin computed in [15] is 0.6198. Using our approach, we can find many stability τ-intervals. If we choose $(k_P = 0.01, k_D = 0.01)$, it corresponds to the second case of Corollary 3 and there are 36 stability τ-intervals and the generalized delay margin is 219.1508. If we choose $(k_P = -0.01, k_D = -0.01)$, it corresponds to the third case of Corollary 4 and there are also 36 stability τ-intervals and the generalized delay margin is 222.2703. ■

In [15], the following assumption is adopted.

Assumption 1: For the controlled plant (20), the controller gains of the PD controller (18) satisfy that $k_P > p_1 p_2$ and $k_D > p_1 + p_2$.

We now present a complete stability analysis of the second-order plant (20) controlled by PD controller (18) using our approach.

Proposition 2: Consider the closed-loop system described by (18) and (20). Under Assumption 1, for Cases U.1, U.2, and U.3, there is one and only one stability τ-interval in the form (3) and the corresponding delay margin $\overline{\tau}$ is finitely large.

Proof: The characteristic function of the closed-loop system when $\tau = 0$ is $f(\lambda, 0) = \lambda^2 + (k_D - p_1 - p_2)\lambda + k_P + p_1 p_2$. Assumption 1 ensures that $k_D - p_1 - p_2 > 0$ and $k_P + p_1 p_2 > 0$ and, hence, both the two characteristic roots are in $\mathbb{C}_-$. Thus, $NU(0) = 0$ in a parameter region where Assumption 1 holds.

The auxiliary characteristic function is $F_{\mathrm{PD}}(W) = W^2 + (p_1^2 + p_2^2 - k_D^2)W + p_1^2 p_2^2 - k_P^2$. Under Assumption 1, $p_1^2 p_2^2 - k_P^2 < 0$ and it is obvious that one W root is positive real while the other one is negative real. Then, we have $\mathcal{N}_W^{\{1,1\}} \to \mathcal{N}_W^{\{\underline{1},\overline{1}\}} \to \mathcal{N}_{W_+}^{\{1\}}$ for a region satisfying Assumption 1.

We can now complete the proof by Corollary 2. ■

According to Proposition 2, the maximal generalized delay margin equals to the maximal delay margin if Assumption 1 is imposed. More precisely, the value is exactly the maximal $\widetilde{\tau}_{0,0}$ in the region, in light of Corollary 2.

Based on the parameter-space approach, we developed a MATLAB toolbox, PID-Design-Delay. It is freely available at http://faculty.neu.edu.cn/ise/lixuguang/PIDCDTDS.html.

The user only needs to input some requisite information through the graphical user interface.[1] The application to Example 11 is shown in Fig. 12.

VIII. Concluding Remarks

In this article, the stabilization of time-delay systems using the PID controller is investigated. All the three controller gains (k_P, k_I, and k_D) and the delay (τ) are treated as free parameters.

First, under given k_P, k_I, and k_D, we develop an algebraic algorithm with which the complete stability analysis w.r.t. τ may be automatically performed through analyzing the $NU(\tau)$ distribution, where $NU(\tau)$ denotes the number of characteristic roots in the right-half plane as a function of τ. As a result, the stability study in the (k_P, k_I, k_D, τ)-space may be recast into the complete stability analysis w.r.t. τ in the (k_P, k_I, k_D)-space.

[1] With the manual and demo videos, an undergraduate can learn to design the PID controller and find the whole stability τ-set in a couple of hours.

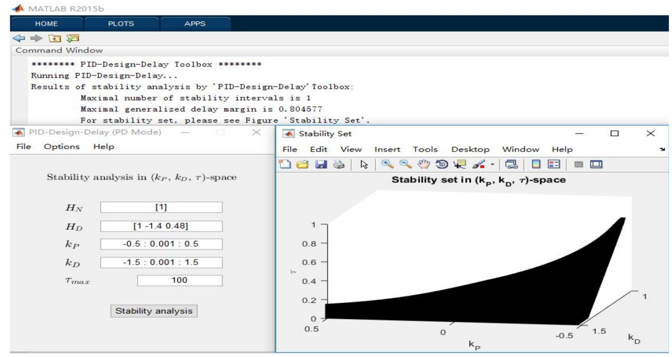

Fig. 12. Application of PID-Design-Delay toolbox.

Second, a procedure for the complete effective W root classification (W is the auxiliary characteristic root) is proposed. With this classification, the (k_P, k_I, k_D)-space may be appropriately divided and all possible abrupt changes of the $NU(\tau)$ distribution can be accurately determined. Third, by specifically taking into account the characteristics of the closed-loop system with PID controller, the procedures for the above local and global analysis can be simplified.

Finally, we establish a new methodology (the new parameter-space approach) for determining the stability set in the (k_P, k_I, k_D, τ)-space, which is systematic from both the theoretical and practical angles.

Appendix A
Proof of Theorem 4

Note that we may label the effective W roots in two forms: (10) and (15). Each W_i^o (W_i^e) in (10) corresponds to $\mathcal{M}_{W_i^o}$ ($\mathcal{M}_{W_i^e}$) elements in (15). Here, $\mathcal{M}_{W_i^o}$ ($\mathcal{M}_{W_i^e}$) denotes the multiplicity of W_i^o (W_i^e), and hence, $\mathcal{M}_{W_i^o}$ ($\mathcal{M}_{W_i^e}$) is an odd (even) number.

With the notations mentioned above, a CIR λ_i^o (λ_i^e) is associated with $\mathcal{M}_{W_i^o}$ ($\mathcal{M}_{W_i^e}$) number of $\widetilde{\lambda}_\alpha$, the set for which is denoted by $\mathbb{S}_{\lambda_i^o}$ ($\mathbb{S}_{\lambda_i^e}$). Furthermore, for a λ_i^o, we denote the corresponding "$(-1)^i$" in (11) by $U_{\lambda_i^o}$ and for a $\widetilde{\lambda}_\alpha$, we denote the corresponding "$(-1)^i$" in (16) by $U_{\widetilde{\lambda}_\alpha}$.

The following two properties are true according to the statement (2) of Theorem 1.

Property 8: If there exists at least one W_i^o in (10), then $U_{\lambda_0^o} = +1$.

Property 9: If there is more than one W_i^o in (10), then for any two consecutive W_i^o, say $W_{i'}^o$ and $W_{i''}^o$, it follows that

$$U_{\lambda_{i'}^o} U_{\lambda_{i''}^o} = -1. \tag{21}$$

Our idea for proving Theorem 4, based on Theorem 2, is to show that the following two conditions always hold

$$U_{\lambda_i^o} = \sum_{\widetilde{\lambda}_\alpha \in \mathbb{S}_{\lambda_i^o}} U_{\widetilde{\lambda}_\alpha} \tag{22}$$

$$0 = \sum_{\widetilde{\lambda}_\alpha \in \mathbb{S}_{\lambda_i^e}} U_{\widetilde{\lambda}_\alpha}. \tag{23}$$

The condition (22) is associated with a λ_i^o (for which $U_{\lambda_i^o} = +1$ or -1) and can be proved by Properties 8 and 9. The condition (23), associated with a λ_i^e, is more obvious.

The proof of Theorem 4 is now complete.

Acknowledgment

The authors wish to thank the Associate Editor and the anonymous reviewers for their constructive comments.

References

[1] B. Alikoç and A. F. Ergenç, "A new delay-independent stability test of LTI systems with single delay," in *Proc. 12th Workshop Time Delay Syst.*, Ann Arbor, MI, USA, 2015, pp. 100–105.

[2] K. J. Åström and T. Hägglund, *PID Controllers: Theory, Design, and Tuning*. Research Triangle Park, NC, USA: Instrument Society of America, 1995.

[3] I. Boussaada and S.-I. Niculescu, "Tracking the algebraic multiplicity of crossing imaginary roots for generic quasipolynomials: A Vandermonde-based approach," *IEEE Trans. Autom. Control*, vol. 61, no. 6, pp. 1601–1606, Jun. 2016.

[4] J. Chen, P. Fu, S.-I. Niculescu, and Z. Guan, "An eigenvalue perturbation approach to stability analysis, Part II: When will zeros of time-delay systems cross imaginary axis?," *SIAM J. Control Optim.*, vol. 48, pp. 5583–5605, 2010.

[5] K. L. Cooke and P. van den Driessche, "On zeros of some transcendental equations," *Funkcialaj Ekvacioj*, vol. 29, pp. 77–90, 1986.

[6] I. I. Delice and R. Sipahi, "Delay-independent stability test for systems with multiple time-delays," *IEEE Trans. Autom. Control*, vol. 57, no. 4, pp. 963–972, Apr. 2012.

[7] K. Gu, V. L. Kharitonov, and J. Chen, *Stability of Time-Delay Systems*. Cambridge, MA, USA: Birkhäuser, 2003.

[8] N. Hohenbichler, "All stabilizing PID controllers for time delay systems," *Automatica*, vol. 45, pp. 2678–2684, 2009.

[9] H. Y. Hu and Z. H. Wang, *Dynamics of Controlled Mechanical Systems With Delayed Feedback*. Berlin, Germany: Springer, 2002.

[10] P. Ju and H. Zhang, "Further results on the achievable delay margin using LTI control," *IEEE Trans. Autom. Control*, vol. 61, no. 10, pp. 3134–3139, Oct. 2016.

[11] X. Li, J.-C. Liu, X.-G. Li, S.-I. Niculescu, and A. Çela, "Reversals in stability of linear time-delay systems: A finer characterization," *Automatica*, vol. 108, Art. no. 108479, 2019.

[12] X.-G. Li, S.-I. Niculescu, and A. Çela, *Analytic Curve Frequency-Sweeping Stability Tests for Systems With Commensurate Delays*. London, U.K.: Springer, 2015.

[13] X.-G. Li, S.-I. Niculescu, A. Çela, L. Zhang, and X. Li, "A frequency-sweeping framework for stability analysis of time-delay systems," *IEEE Trans. Autom. Control*, vol. 62, no. 8, pp. 3701–3716, Aug. 2017.

[14] X.-G. Li, L. Zhang, X. Li, and J.-X. Chen, "Colored stability crossing sets for SISO delay systems," *IEEE Trans. Autom. Control*, vol. 63, no. 11, pp. 4016–4023, Nov. 2018.

[15] D. Ma and J. Chen, "Delay margin of low-order systems achievable by PID controllers," *IEEE Trans. Autom. Control*, vol. 64, no. 5, pp. 1958–1973, May 2019.

[16] D. Ma, J. Chen, A. Liu, J. Chen, and S.-I. Niculescu, "Explicit bounds for guaranteed stabilization by PID control of second-order unstable delay systems," *Automatica*, vol. 100, pp. 407–411, 2019.

[17] W. Michiels, I. Boussaada, and S.-I. Niculescu, "An explicit formula for the splitting of multiple eigenvalues for nonlinear eigenvalue problems, and connections with the linearization for the delay eigenvalue problem," *SIAM J. Matrix Anal. Appl.*, vol. 38, pp. 599–620, 2017.

[18] W. Michiels, "Spectrum based stability analysis and stabilization of systems described by delay differential algebraic equations," *IET Control Theory Appl.*, vol. 5, pp. 1829–1842, 2011.

[19] W. Michiels, K. Engelborghs, P. Vansevenant, and D. Roose, "The continuous pole placement method for delay equations," *Automatica*, vol. 38, pp. 747–761, 2002.

[20] W. Michiels and S.-I. Niculescu, *Stability, Control, and Computation for Time-Delay Systems: An Eigenvalue-Based Approach*. Philadelphia, PA, USA: SIAM, 2014.

[21] W. Michiels, T. Vyhlídal, and P. Zítek, "Control design for time-delay systems based on quasi-direct pole placement," *J. Process Control*, vol. 20, pp. 337–343, 2010.

[22] R. H. Middleton and D. E. Miller, "On the achievable delay margin using LTI control for unstable plants," *IEEE Trans. Autom. Control*, vol. 52, no. 7, pp. 1194–1207, Jul. 2007.

[23] C.-I. Morărescu, C.-F. Méndez-Barrios, S.-I. Niculescu, and K. Gu, "Stability crossing boundaries and fragility characterization of PID controllers for SISO systems with I/O delays," in *Proc. Amer. Control Conf., San Francisco*, CA, USA, 2011, pp. 4988–4993.

[24] J. Neimark, "D-Subdivisions and spaces of quasi-polynomials," *Prikl. Mat. Meh.*, vol. 13, pp. 349–380, 1949.

[25] P. M. Nia and R. Sipahi, "Controller design for delay-independent stability of linear time-invariant vibration systems with multiple delays," *J. Sound Vib.*, vol. 332, pp. 3589–3604, 2013.

[26] N. Olgac and R. Sipahi, "An exact method for the stability analysis of time-delayed linear time-invariant (LTI) systems," *IEEE Trans. Autom. Control*, vol. 47, no. 5, pp. 793–797, May 2002.

[27] L.-L. Ou, W.-D. Zhang, and L. Yu, "Low-order stabilization of LTI systems with time delay," *IEEE Trans. Autom. Control*, vol. 54, no. 4, pp. 774–787, Apr. 2009.

[28] T. Qi, J. Zhu, and J. Chen, "Fundamental limits on uncertain delays: When is a delay system stabilizable by LTI controllers?," *IEEE Trans. Autom. Control*, vol. 62, no. 3, pp. 1314–1328, Mar. 2017.

[29] G. J. Silva, A. Datta, and S. P. Bhattacharyya, *PID Controllers for time-delay Systems*. Boston, MA, USA: Birkhäuser, 2005.

[30] K. Walton and J. E. Marshall, "Direct method for TDS stability analysis," *Proc. IEE, Part D—Control Theory Appl.*, vol. 134, pp. 101–107, 1987.

[31] H. Wang, J. Liu, and Y. Zhang, "New results on eigenvalue distribution and controller design for time delay systems," *IEEE Trans. Autom. Control*, vol. 62, no. 6, pp. 2886–2901, Jun. 2017.

[32] Z. H. Wang and H. Y. Hu, "Stability switches of time-delayed dynamic systems with unknown parameters," *J. Sound Vib.*, vol. 233, pp. 215–233, 2000.

[33] L. Yang, "Recent advances on determining the number of real roots of parametric polynomials," *J. Symbolic Comput.*, vol. 28, pp. 225–242, 1999.

Xu-Guang Li was born in Shenyang, Liaoning, China, in 1980. He received the Ph.D. degree in automatic control from Shanghai Jiaotong University, Shanghai, China, in 2008.

He was a Postdoctoral with ESIEE, Paris, France, and CNRS-Supélec, France, in 2008 and 2009. In 2010, he joined Northeastern University, Shenyang, China, where he is currently a Full Professor. He has coauthored three books: *Optimal Design of Distributed Control and Embedded Systems* (with A. Çela, M. Ben Gaid, and S.-I. Niculescu, Springer, 2014); *Analytic Curve Frequency-Sweeping Stability Tests for Systems With Commensurate Delays* (with S.-I. Niculescu and A. Çela, Springer, 2015); and *Complete Stability Analysis for Time-Delay Systems: A Frequency-Sweeping Mathematical Framework* (to be submitted to Springer). His main research interests include the stability and stabilization of time-delay systems, the application of analytic-curve perspective to control systems, and the development of stability analysis toolboxes for time-delay systems.

Silviu-Iulian Niculescu (Fellow, IEEE) received the B.S. degree in automatic control from the Polytechnical Institute of Bucharest, Bucharest, Romania, in 1992, the M.Sc. and Ph.D. degrees in automatic control from the Institut National Polytechnique de Grenoble, Grenoble, France, in 1993 and 1996, respectively, and the French Habilitation (HDR) degree in automatic control from Université de Technologie de Compièone, in 2003.

He is currently a Research Director with CNRS (French National Center for Scientific Research) and the Head of L2S (Laboratory of Signals and Systems), a joint research unit of CNRS with CentraleSupelec, Gif-sur-Yvette, France, and Université Paris-Sud. Gif-sur-Yvette, France. He is the author/co-author of ten books and of more than 500 scientific papers. His research interests include delay systems, robust control, operator theory, and numerical methods in optimization, and their applications to the design of engineering systems.

Dr. Niculescu was the recipient of a Doctor Honoris Causa of University of Craiova, Romania, in 2016, and the CNRS Bronze and Silver Medals in 2001 and 2011, respectively. He is the Chair of the IFAC (International Federation of Automatic Control) Technical Committee "Control Linear Systems" since 2017. He has been the Founding Editor and the Editor-in-Chief of the Springer Nature Series "*Advances in Delays and Dynamics*" since 2012.

Jun-Xiu Chen was born in Linyi, Shandong, China, in 1992. She received the B.S. degree in mathematics and applied mathematics from Linyi University, Linyi, China, in 2015, and the M.S. degree in mathematics in 2017 from Northeastern University, Shenyang, China, where she is currently working toward the Ph.D. degree in automatic control.

Her main research interests include the stability and stabilization of time-delay systems by using the frequency-sweeping mathematical framework and the application of analytic-curve perspective to control systems.

Tianyou Chai (Fellow, IEEE) received the Ph.D. degree in control theory and engineering from the Northeastern University, Shenyang, China, in 1985.

In 1988, he became a Professor with the Northeastern University, where he became a Chair Professor in 2004. He is the Founder and Director of the Center of Automation, which became a National Engineering and Technology Research Center and a State Key Laboratory. His current research interests include modeling, control, optimisation, and integrated automation of complex industrial processes.

Dr. Chai is a member of the Chinese Academy of Engineering, an Academician of the International Eurasian Academy of Sciences, and an IFAC Fellow. He is a Distinguished Visiting Fellow of The Royal Academy of Engineering (United Kingdom) and an Invitation Fellow of Japan Society for the Promotion of Science (JSPS).